Generalized Surface Interpolation for Triangle Meshes with Feature Retention

Yi Su[1] and A. Senthil Kumar[2]

[1]Institute of High Performance Computing, suyi@ihpc.a-star.edu.sg
[2]National University of Singapore, mpeask@nus.edu.sg

ABSTRACT

In this paper, a local surface interpolation scheme for triangle meshes based on a quartic triangular Bezier patch is presented. This work extends previous research in surface interpolation to cater for any arbitrary node configuration with special focus on feature retention. The approach involves a hierarchical feature identification process which extracts all the feature edges and nodes. Based on this feature hierarchy, the nodal normal and tangent vectors are defined and used as input parameters for the surface interpolation. Finally, the control points of the Bezier patch is calculated by modifying the Walton scheme. Results show that the geometrical approximation is significantly improved using this surface interpolation scheme in a remeshing context. Strict feature retention is also achieved with good shape approximation.

Keywords: Surface interpolation; Quartic Bezier patch; Feature retention; Triangle mesh.

1. INTRODUCTION

Computer Aided Engineering (CAE) processes have primarily been relying on geometric models as the basis to generate the analysis model for simulation. However, due to the evolution of the simulation problem and the methodology of data acquisition, an underlying geometry might not be always available. For example, data acquisition using range scanners and extracting isosurfaces from volume datasets generally produce polygonized models rather than geometric models. Also, due to the large physical deformation associated with some dynamic analysis, the original geometry becomes inappropriate should the need for remeshing arise.

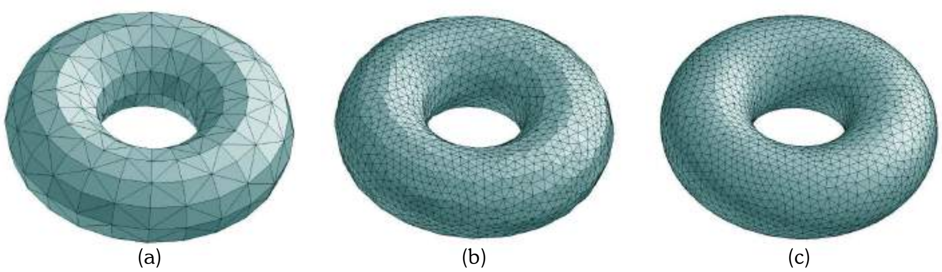

Fig. 1. Example of a torus showing (a) the base mesh, (b) result of remeshing using simple projection and (c) result of remeshing using surface interpolation

It was not surprising that various commercial CAE solution providers began to introduce meshing algorithms that utilizes triangulated data as pseudo geometry for mesh generation. For example, MSC.Patran [9] has introduced a remeshing code, called the mesh-on-mesh method, as a beta feature in its 2001 release. This has been subsequently included as one of the mainstream mesh generation feature in its later releases. However, a common problem associated with this method is in the creation of new nodes which is based on normal projection onto the original triangulated geometry. This simplistic approach is sufficient if the underlying geometry is planar, but high geometrical inaccuracy can be introduced if the curvature is high. In Fig. 1(a), a coarse base mesh of a torus is used to illustrate this. Using a simplistic projection approach, visual faceting is observed in Fig. 1(b) as the resulting mesh approximates the original geometry badly. It would, thus, be desirable that the underlying geometry is approximated from the base mesh so that a mesh with better geometrical conformity can be obtained, as shown in Fig. 1(c).

One way to achieve this is by employing surface interpolation techniques. There are a variety of computationally light-weight surface fitting algorithms proposed by Vlachos et al. [17], Lee and Jen [6,7] and van Overveld and Wyvill [16]. While these are suitable in the field of computer graphics where special display techniques are used to conceal the lack of G^1 continuity, a more stringent criterion is often required for CAE applications. In this work, we consider the quartic Bezier patch as a viable candidate for surface interpolation as it has been established that for G^1 continuity, the minimum degree of the triangular Bezier patch is 4 [11]. Walton and Meek [19] has initiated work in this area, which assumes that the triangles transit smoothly across every edge. This is not realistic for engineering purposes where hard edges and features are commonplace. A later development by Owen et al. [10] extends the scheme to include sharp edges but this is restricted to nodes which are of degree 2. Again, this is rather restrictive where engineering modeling is concerned.

In our work, the objective is to extend the surface interpolation scheme to include nodes of any arbitrary degree. Essentially, this would generalize the surface interpolation scheme to cater to any geometric configuration. The focus here is to ensure that there are smooth transitions *across* every non-feature edge while the variations of tangent *along* connected feature edges are smooth. This principle forms the basis of feature retention.

The rest of the paper is organized as follows: Section 2 gives the overview of the methodology used to perform the surface fitting based on a quartic Bezier patch. A robust treatment of feature edges and vertices is detailed in the next section. The derivations of the unique nodal normal and tangent vectors are also described here. This is followed by a presentation of the modified Walton scheme, given the additional input parameters. Section 5 presents some examples and results of the algorithm before concluding in Section 6.

2. METHODOLOGY

The new proposed scheme to fit a quartic triangular Bezier patch over a triangle face presented here is an extension of the theorem established by Walton and Meek [19], which assumes G^1 continuity across every edge. In the subsequent work by Owen et al. [10], special treatment is administered to define the parameters at feature edges. However, the case is only confined to nodes with degree 2. The contribution of our work generalized the surface interpolation scheme so that features of the mesh are modeled accurately for any arbitrary configuration.

There are 3 main steps involved in the feature retaining surface interpolation scheme:

(1) *Feature extraction*. This involves querying the model for edges and nodes that form the features of the model, and classifying them in a hierarchical manner.

(2) *Definition of normal and tangent vectors*. This involves calculating the 3 nodal normal vectors and the 6 nodal tangent vectors based on the feature hierarchy of the entity.

(3) *Surface interpolation*. This involves calculating the control points for the quartic triangular Bezier patch based on a modification of the Walton scheme.

The subsequent sections detail how these steps are performed.

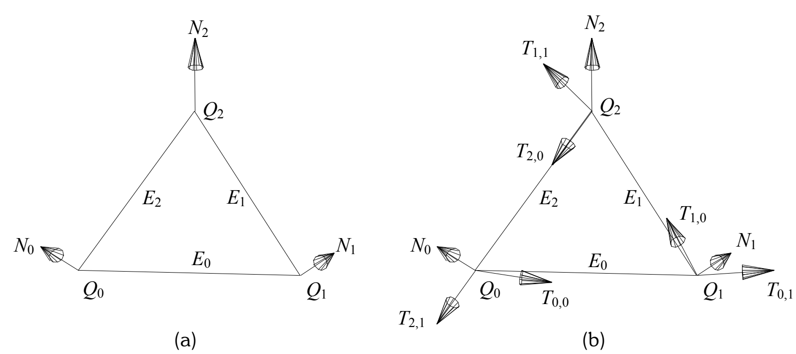

Fig. 2. Input parameters for surface interpolation based on (a) Walton's scheme and (b) new proposed scheme

3. FEATURE RETENTION

Careful treatment of feature edges is vital to ensure that the shape is modeled accurately and that there are no gaps along these edges as a result of the surface fitting. Essentially, G^1 conditions are required *across* non feature edges whereas tangents are modeled continuously *along* feature edges. In order to achieve this, additional input parameters are included in the formulation of the Bezier patch, namely, the inclusion of six nodal tangent vectors for each triangle face. This is contrasted with the input parameters required for Walton's patch fitting procedure, as shown in Fig. 2. In order to derive these input parameters, a feature extraction procedure is performed.

3.1 Feature extraction

The key to feature retention in our surface interpolation scheme lies in the appropriate definition of nodal normal vectors and nodal tangent vectors at the vertices of the edges. With this in view, a feature extraction routine is required to determine all the feature edges and feature nodes of the mesh. The heuristics are summarized as follows:

(1) An edge is considered a *boundary feature* if it is only associated to one adjacent face.
(2) An edge is considered an *internal feature* if the faces adjacent to it form an interior angle smaller than a given angular tolerance θ_e.
(3) An edge is considered *non-feature* otherwise.

After the classification of the edges, the corresponding nodes are classified based on the following:

(1) A node is an *interior* node if there are no associated feature edges connected to it.
(2) A node is a *feature* node if it is connected to at least one feature edge.
(3) A node is considered a *vertex* node if
- it is connected to only one feature edge (i.e. degree = 1), or
- it is connected to more than two feature edges (i.e. degree = 2), or
- it is connected to two feature edges with an angle less than a given angular tolerance θ_e.

(4) An interior node is considered an *apex* node if it does not satisfy the angle deficit criteria [8], that is, the sum of angles about the node is less than a prescribed limiting apex angle θ_α.

3.2 Approximation of nodal normal vectors

As mentioned, the necessary input parameters are the three nodal coordinates Q_i, the three nodal normal vectors N_i and the six tangent vectors $T_{i,j}$ where $i = \{0,1,2\}$ and $j = \{0,1\}$, as shown in Fig. 2(b). Note that the tangent vector at the node is unique with respect to each edge.

The nodal nodal normal vector (see Fig. 3) is determined based on the following three cases:

(1) If the node is an *interior* node or if the node is a *feature* node with degree one, the nodal normal vector N is the average of the normal vectors of its associated face weighted against the incident angle

$$N = \frac{\sum_{i=1}^{n} \alpha_i N_i}{\sum_{i=1}^{n} \alpha_i} \tag{1}$$

where N_i is the face normal vector and α_i the incident angle.

(2) If the node is a *feature* node with degree greater than one, the nodal normal vector N is the average of the normal vectors of a subset of its associated face weighted against the incident angle. This subset is such that the faces do not traverse across a feature edge, as shown in Fig. 3(b).
(3) If the node is an *apex* node, the nodal normal vector N is simply the normal of the face under consideration, as shown in Fig. 3(c).

3.3 Approximation of nodal tangent vectors

As the nodal tangent vectors are calculated with respect to the edges, the consideration of the edge type is crucial. The following heuristic is used to determine the nodal tangent vectors $T_{i,j}$ of Face F:

(1) If the edge is a *non-feature* edge, or if it is a *boundary* edge, or if it is an *internal feature* edge and the node in consideration is of degree 1, the nodal tangent is merely the edge vector such that

$$T_{i,j} = \frac{Q_{i+1} - Q_i}{\left\| Q_{i+1} - Q_i \right\|} \qquad (2)$$

(2) If the edge is a *boundary* edge and the node in consideration is of degree 2, the nodal tangent is the average of the edge vectors of the 2 boundary edges.

(3) If the edge is an *internal feature* edge and the node in consideration is of degree greater than 1, the nodal tangent is obtained from the cross product of the normal vector of F with the normal vector of the adjacent face F_{adj} sharing this edge such that

$$T_{i,j} = \frac{N \times N_{adj}}{\left\| N \times N_{adj} \right\|} \qquad (3)$$

Since the tangents vectors are obtained from information provided from the adjacent faces, the control polygon for the boundary curve representing the feature edge is the same for both faces F and F_{adj}, thus ensuring C^0 continuity.

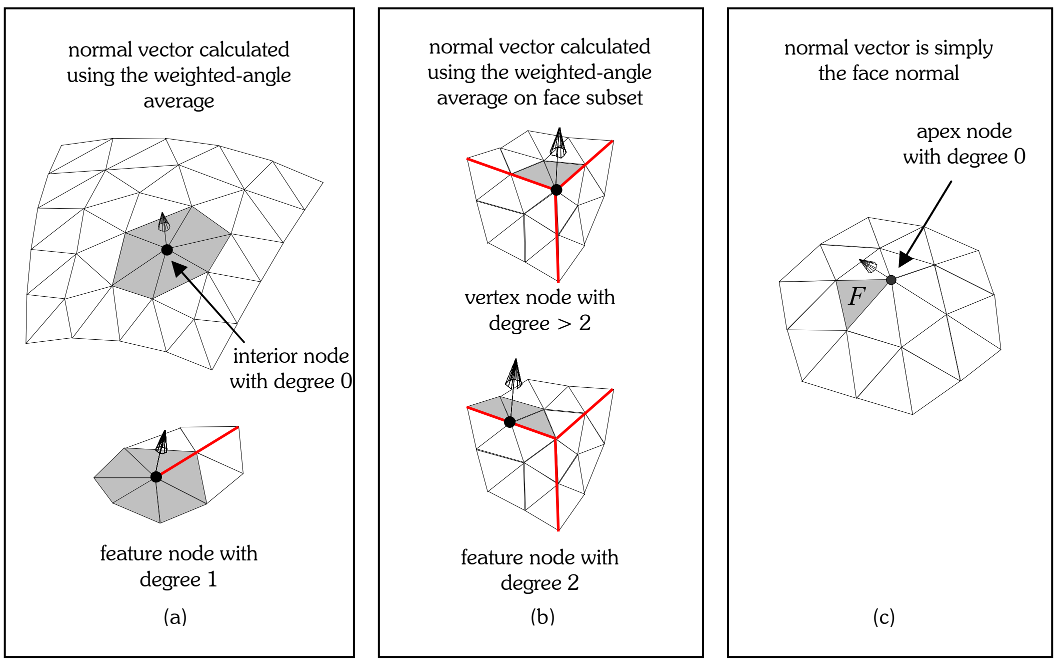

Fig. 3. Determining the nodal normal vector

4. SURFACE INTERPOLATION

The procedure to derive a suitable surface interpolation is generalized into two parts. Firstly, the edges of the triangular face are approximated using quartic Bezier curves. Secondly, the interior control points of the quartic Bezier patch are determined. Fig. 4(a) illustrates the control points of the Bezier patch. Once all the control points $P_{i,j,k}$ are determined, the patch can be described by

$$S(u,v,w) = \sum_{i+j+k=4} P_{i,j,k} \frac{4!}{i!\,j!\,k!} u^i v^j w^k \qquad (4)$$

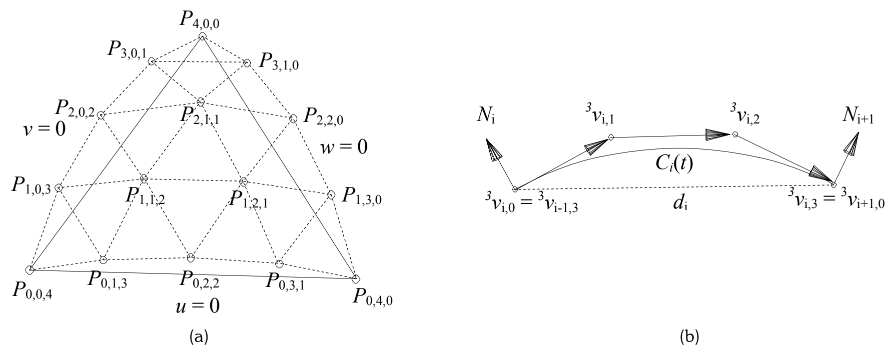

Fig. 4. Control points of (a) a quartic triangular Bezier patch and (b) a boundary cubic Bezier curve

4.1 Approximating boundary curves

The control vertices of the cubic Bezier boundary curve ${}^3C_i(t)$ can be obtained using a point normal interpolation [18]. To ensure that the feature edges are modeled correctly, modifications are made to Walton's formulation to reflect the usage of unique nodal tangent vectors at the vertices of each boundary curve. Given that $d_i = \|Q_{i+1} - Q_i\|$, $a_i = N_i \cdot N_{i+1}$, $a_{i,0} = N_i \cdot T_{i,0}$ and $a_{i,1} = N_{i+1} \cdot T_{i,1}$, the control vertices ${}^3v_{i,j}$ (see Fig. 3(b)) are calculated based on the following equations:

$$ {}^3v_{i,0} = Q_i \tag{5} $$

$$ {}^3v_{i,3} = Q_{i+1} \tag{6} $$

$$ {}^3v_{i,1} = Q_i + \frac{d_i(6T_{i,0} - 2\rho_i N_i + \sigma_i N_{i+1})}{18} \tag{7} $$

$$ {}^3v_{i,2} = Q_{i+1} - \frac{d_i(6T_{i,1} + \rho_i N_i - 2\sigma_i N_{i+1})}{18} \tag{8} $$

where $\rho_i = \dfrac{6(2a_{i,0} + a_i a_{i,1})}{4 - a_i^2}$ and $\sigma_i = \dfrac{6(2a_{i,1} + a_i a_{i,0})}{4 - a_i^2}$.

Since the interest is to approximate the triangle with a quartic triangular Bezier patch, the degree of the cubic boundary curve ${}^3C_i(t)$ must be elevated to form a quartic Bezier curve ${}^4C_i(t)$ with control vertices given by

$$ {}^4v_{i,j} = \tfrac{1}{4}\left(j({}^3v_{i,j-1}) + (4-j)({}^3v_{i,j}) \right) \tag{9} $$

where j = {0, 1, 2, 3, 4}. Then, the control points of the boundary curves of the quartic triangular Bezier patch are given by

$$ P_{o,j,4-j} = {}^4v_{0,j}, \quad P_{j,4-j,0} = {}^4v_{1,j}, \quad P_{4-j,0,j} = {}^4v_{2,j} \tag{10} $$

4.2 Determining interior control points

Next, to define the interior control points $P_{1,1,2}$, $P_{1,2,1}$ and $P_{2,1,1}$ of the quartic triangular Bezier patch, the control points adjacent to a boundary curve are derived by imposing tangential continuity constraints across that boundary. Since each interior control point is associated with two boundary curves, it is determined twice, yielding two different locations $G_{i,1}$ and $G_{i,2}$. These are then blended to give the interior control point by ensuring tangential plane continuity across each associated boundary. The locations of $G_{i,1}$ and $G_{i,2}$ are obtained by

$$G_{i,1} = \tfrac{1}{8}\left({}^3v_{i,0} + 5({}^3v_{i,1}) + 2({}^3v_{i,2})\right) + \tfrac{2}{3}\lambda_{i,0}w_{i,1} + \tfrac{1}{3}\lambda_{i,1}w_{i,0} + \tfrac{2}{3}\mu_{i,0}A_{i,1} + \tfrac{1}{3}\mu_{i,1}A_{i,0} \quad (11)$$

$$G_{i,2} = \tfrac{1}{8}\left(2({}^3v_{i,1}) + 5({}^3v_{i,2}) + v_{i,3}\right) + \tfrac{1}{3}\lambda_{i,0}w_{i,2} + \tfrac{2}{3}\lambda_{i,1}w_{i,1} + \tfrac{1}{3}\mu_{i,0}A_{i,2} + \tfrac{2}{3}\mu_{i,1}A_{i,1} \quad (12)$$

where $w_{i,k} = {}^3v_{i,k+1} - {}^3v_{i,k}$, $A_{i,0} = \dfrac{N_i \times w_{i,0}}{\left\|w_{i,0}\right\|}$, $A_{i,2} = \dfrac{N_{i+1} \times w_{i,2}}{\left\|w_{i,2}\right\|}$ and $A_{i,1} = \dfrac{A_{i,0} + A_{i,2}}{\left\|A_{i,0} + A_{i,2}\right\|}$ for $\{i = 0, 1, 2\}$.

The parameters λ and μ are calculated from

$$\lambda_{i,0} = \frac{D_{i,0} \cdot w_{i,0}}{w_{i,0} \cdot w_{i,0}}, \quad \lambda_{i,1} = \frac{D_{i,3} \cdot w_{i,2}}{w_{i,2} \cdot w_{i,2}} \quad (13)$$

$$\mu_{i,0} = D_{i,0} \cdot A_{i,0}, \quad \mu_{i,1} = D_{i,3} \cdot A_{i,2} \quad (14)$$

where

$$D_{0,j} = P_{1,j,3-j} - \tfrac{1}{2}\left(P_{0,j+1,3-j} + P_{0,j,4-j}\right) \quad (15)$$

$$D_{1,j} = P_{j,3-j,1} - \tfrac{1}{2}\left(P_{j+1,3-j,0} + P_{j,4-j,0}\right) \quad (16)$$

$$D_{2,j} = P_{3-j,1,j} - \tfrac{1}{2}\left(P_{3-j,0,j+1} + P_{4-j,0,j}\right) \quad (17)$$

for {j = 0, 3}.

Finally, the interior control points for the quartic triangular Bezier patch are given by

$$\begin{aligned} P_{1,1,2} &= \frac{1}{u+v}\left(uG_{2,2} + vG_{0,1}\right) \\ P_{1,2,1} &= \frac{1}{w+u}\left(wG_{0,2} + uG_{1,1}\right) \\ P_{2,1,1} &= \frac{1}{v+w}\left(vG_{1,2} + wG_{2,1}\right) \end{aligned} \quad (18)$$

Now that all the control points are determined, the quartic triangular Bezier patch can be obtained from Eqn. (4).

5. RESULTS AND DISCUSSIONS

In this section, a study is performed to verify the improvement in the geometric fit when our surface interpolation scheme is employed in a remeshing algorithm. In order to have a quantifiable means to conduct an error analysis, a geometric model of a curved panel is used. As shown in Fig. 5, this model consists of a set of trimmed free-formed surfaces with concave and convex features, as well as hard vertices. From this model, an initial base mesh is constructed to act as the input to the remeshing routine.

The comparison is made between the mesh-on-mesh feature of MSC.Patran [9], which is a commercial 3D mechanical computer-aided engineering (MAE) software package, and the same remeshing engine but with our surface interpolation capability. The remeshing routine is basically an advancing front algorithm which uses an existing mesh as the underlying geometry. For readers who are interested, the authors recommend [1-4]. While there are other remeshing schemes available [5,12-15], we use the advancing front method in this paper for the sake of comparison and for the fact that quadrilateral elements are supported. It is observed that the former produces a mesh with visually faceted regions owing to the fact that the new nodal points are projected onto the planar faces of the base mesh. The faceting effect is more pronounced when the area of the base triangle is larger than the target mesh size. Also, the mesh along the boundary edges is poor due to linear interpolation. However, with surface interpolation, the new mesh conforms to a smoothly varying profile which matches that of the original geometry. Fig. 5 also illustrates that at curved boundary edges, the mesh conforms smoothly even though the base mesh was modeled with poor resolution.

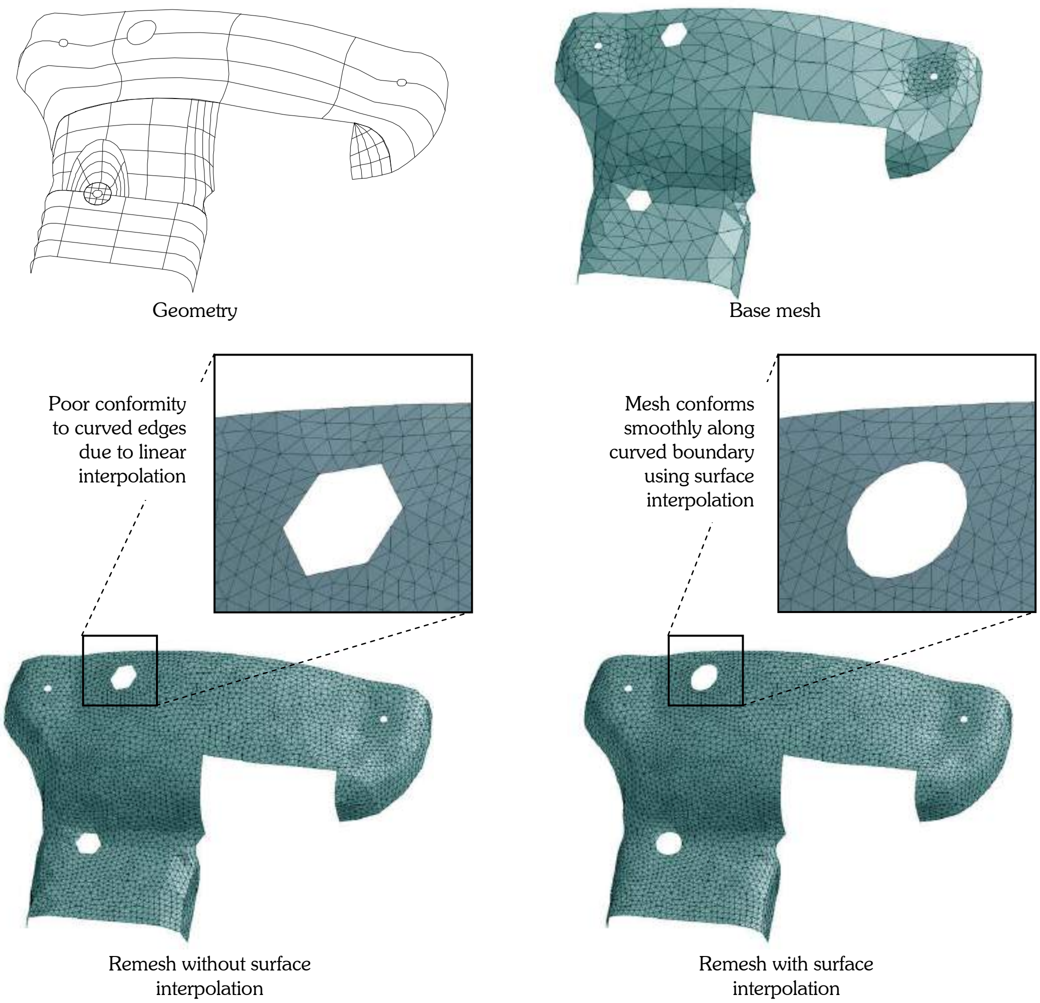

Fig. 5. Comparison of mesh-on-mesh operations on panel model

To further quantify the results, an error analysis is performed by calculating the absolute normal projected distance of the new nodes to the original geometry. In Fig. 6, it was observed that the geometric error is significantly greater without using the surface interpolation scheme. At regions with high curvature and low base mesh resolution, the error tends to be much higher. However, using surface interpolation, the geometric error is significantly reduced. Fig. 7 plots the histogram of the geometric errors. Note that with surface interpolation, 98% of the nodes have geometric error of less than 1.0. This is significantly better as compared to the case without surface interpolation, where only 86% of the nodes have geometric error of less than 1.0. Also, the maximum error for the scheme without surface interpolation is 4.14 as compared to 3.26 for the case using interpolation.

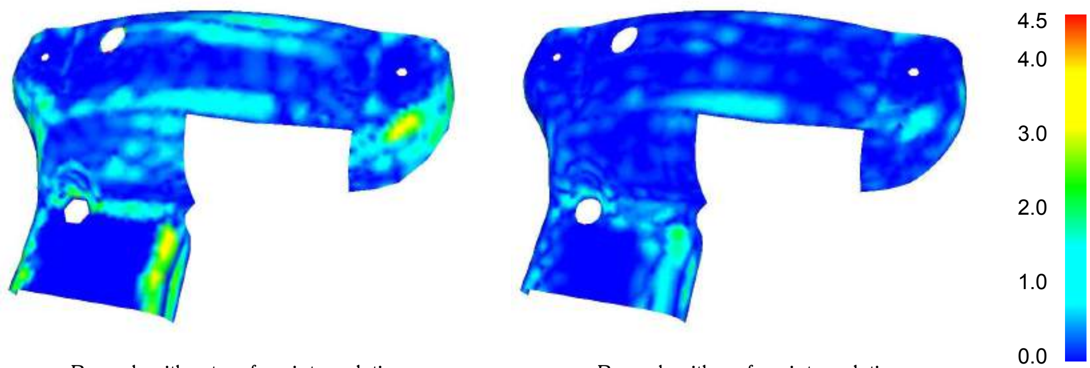

Remesh without surface interpolation Remesh with surface interpolation

Fig. 6. Plot of geometric errors for panel meshes

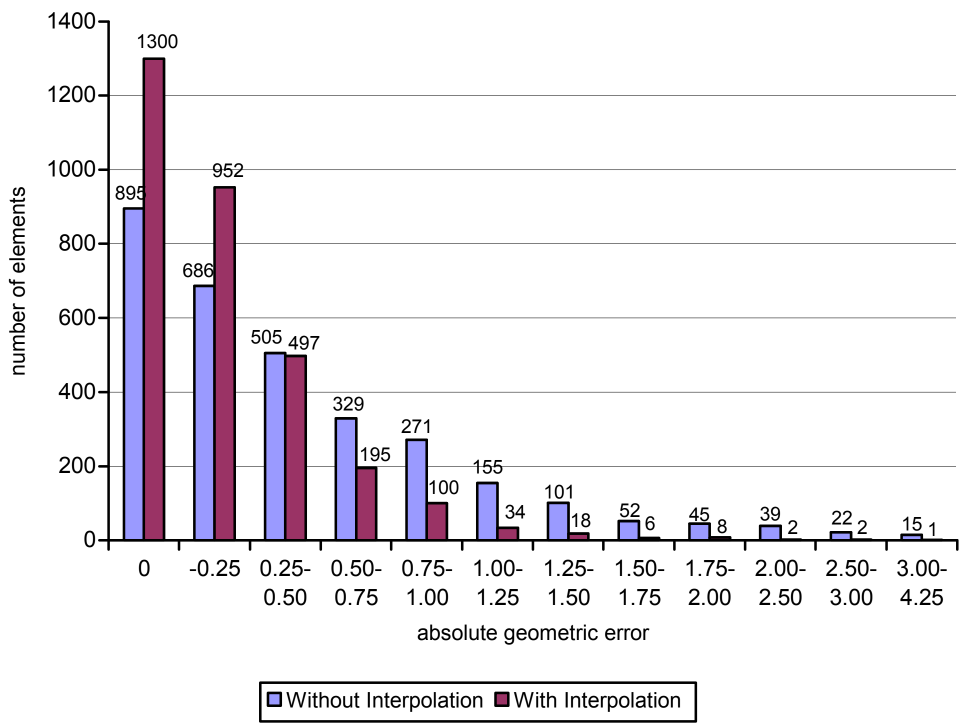

Fig. 7. Error analyses of remeshing schemes

Next, an example of a coarse aerofoil mesh is used to illustrate the ability of the surface interpolation scheme to model nodes with degree greater than 2. As shown in Fig. 8, the vertex of the trailing edge of the aerofoil is of degree 3. Note that the mesh conforms smoothly along the feature edges and terminates at the sharp vertex. Given that the profile of the base mesh is of an overly coarse resolution, a finer mesh with better geometrical fit can be obtained with strict feature retention using our surface interpolation scheme. It is also worthy to mention that the remeshing scheme with surface interpolation is not restricted to triangular elements but also quadrilateral. In fact, higher order elements can be similarly used for the remeshing process, like quadratic triangular and quadratic quadrilateral elements. Lastly, a more complex model of a cutter is used to illustrate the robustness of our method, as shown in Fig. 9.

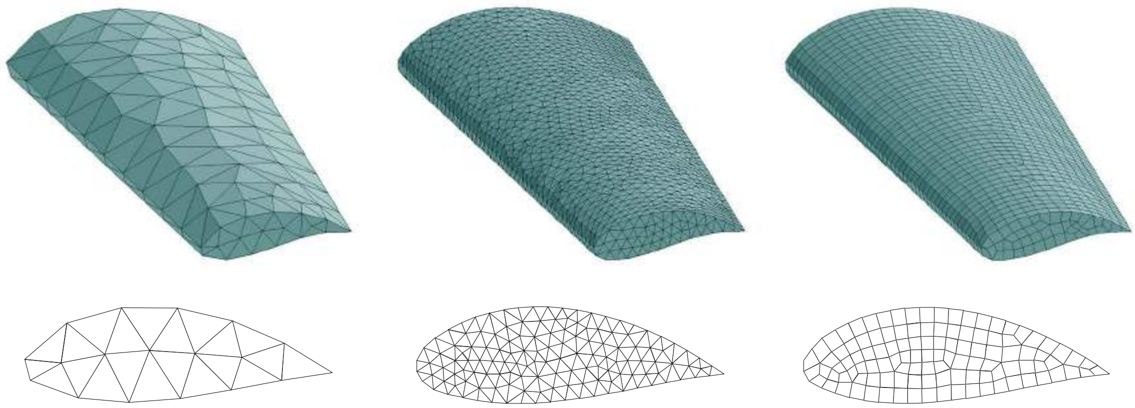

Base mesh

Remesh with surface interpolation (triangles)

Remesh with surface interpolation (quadrilaterals)

Fig. 8. Example of aerofoil model

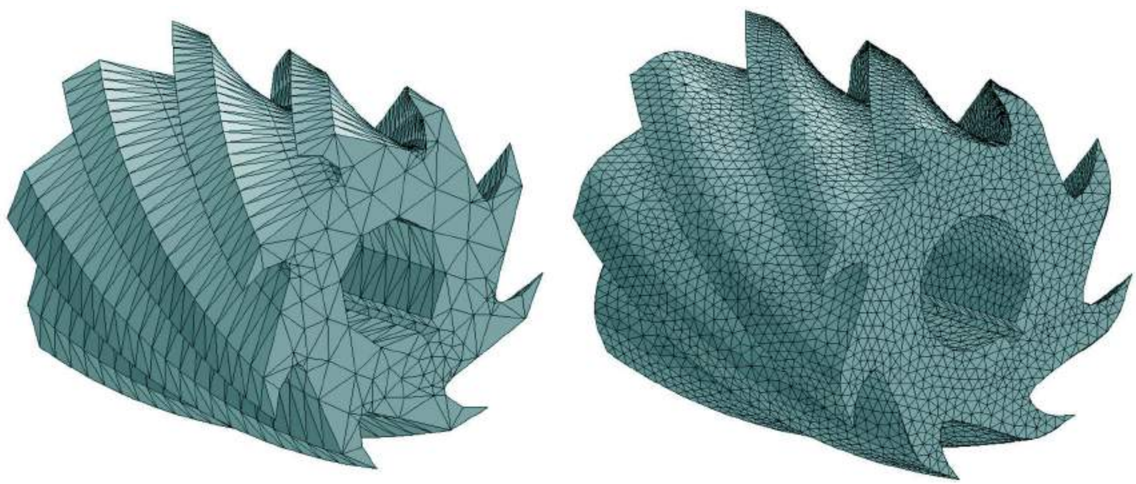

Base mesh

Remesh with surface interpolation

Fig. 9. Example of cutter model

6. CONCLUSIONS

In this work, an improved surface interpolation scheme based on a quartic triangular Bezier patch is proposed which has robust feature retaining capability. The key to approximating a polygonized model lies in the appropriate definitions of nodal normal and tangent vectors based on the feature hierarchy presented. Using such an approach allows smooth transitions across non-feature edges while the mesh along connected feature edges are smoothly modeled. In a remeshing context, our surface interpolation scheme achieves significant improvement in terms of geometric approximation and shape conformity.

7. REFERENCES

[1] Blacker, T.D. and Stephenson, M.B., Paving: A new approach to automated quadrilateral mesh generation. *International Journal for Numerical Methods in Engineering*, 1991, Vol. 32, pp 811-847.

[2] Borouchaki, H., Laug, P. and George, P.L., Parametric surface meshing using a combined advancing-front generalized Delaunay approach. *International Journal for Numerical Methods in Engineering*, 2000, Vol. 49, No. 1, pp 233-259.

[3] Cass, R.J., Generalized 3D paving: An automated quadrilateral surface mesh generation algorithm. *International Journal for Numerical Methods in Engineering*, 1996, Vol. 39, No. 9, pp 1475-1489.

[4] Cuilliere, J.C., An adaptive method for the automatic triangulation of 3D parametric surfaces. *Computer-Aided Design*, 1998, Vol. 30, No. 2, pp 139-149.

[5] Frey, P.J., About surface remeshing. *Proceedings, 9th International Meshing Roundtable, Sandia National Laboratories*, 2000, pp 123-136.

[6] Lee, Y.-C. and Jen, C.-W., Improved quadratic normal vector interpolation for realistic shading. *The Visual Computer*, 2001, Vol. 17, No. 6, pp 337–352.

[7] Lee, Y.-C. and Jen, C.-W., On-Line polygon refining using a low computation subdivision algorithm. *Proceedings of Geometrical Modeling and Processing, Hong Kong*, 2000, pp 209-219.

[8] Meek, D.S. and Walton, D.J., On surface normal and Gaussian curvature approximations given data sampled from a smooth surface. *Computer Aided Geometric Design*, Vol. 17, No. 6, 2000, pp 521-543.

[9] MSC.Patran, http://www.mscsoftware.com/, MSC Software.

[10] Owen, S.J., White, D.R. and Tautges, T.J., Facet-based surfaces for 3D mesh generation. *Proceedings, 11th International Meshing Roundtable, Sandia National Laboratories*, 2002, pp 297-312.

[11] Piper, B., Visually smooth interpolation with triangular Bezier patches. In: Farin, G. (Ed.) *Geometric Modelling: Algorithms and New Trends*, SIAM, Philadelphia, 1987, pp 221-233.

[12] Rassineux, A., Villon, P., Savignat, J.-M.. and Stab, O., Surface remeshing by local hermite diffuse interpolation. *International Journal for Numerical Methods in Engineering*, 2000, Vol. 49, No. 1, pp 31-49.

[13] Sifri, O., Sheffer, A. and Gotsman, C., Geodesic-based surface remeshing. *Proceedings, 12th International Meshing Roundtable, Sandia National Laboratories*, 2003, pp 189-199.

[14] Surazhsky, V., Alliez, P. and Gotsman, C., Isotropic remeshing of surfaces: a local parameterization approach. *Proceedings, 12th International Meshing Roundtable, Sandia National Laboratories*, 2003, pp 215-224.

[15] Surazhsky, V. and Gotsman, C., Explicit surface remeshing. *Proceedings of Eurographics Symposium on Geometry Processing*, 2003, pp 17-28.

[16] van Overveld, C. and Wyvill, B., An algorithm for polygon subdivision based on vertex normals. *Computer Graphics International*, 1997, pp 3–12.

[17] Vlachos, A., Peters, J., Boyd, C. and Mitchell, J.L., Curved PN triangles. *Proceedings of the 2001 symposium on Interactive 3D graphics*, 2001, pp 159-166.

[18] Walton, D.J. and Yeung, M., Geometric modelling from CT scans for stereolithography apparatus. In: Tang, Z. (Ed.) *New Advances in CAD & Computer Graphics (Proc. CAD/Graphics '93)* International Academic Publishers, Beijing, China, 1993, pp 417-422.

[19] Walton, D.J. and Meek, D.S., A triangular G^1 patch from boundary curves. *Computer-Aided Design*, Vol. 28, No. 2, 1996, pp 113-123.